



Published in final edited form as:

Circ Res. 2023 March 31; 132(7): 867–881. doi:10.1161/CIRCRESAHA.122.321583.

## β3AR-Dependent BDNF Generation Limits Chronic Post-Ischemic Heart Failure

Alessandro Cannavo, PhD<sup>1,2,\*</sup>, Seungho Jun, MD<sup>3,\*</sup>, Giuseppe Rengo, MD, PhD<sup>1,4,\*</sup>, Federica Marzano, PhD<sup>1,2</sup>, Jacopo Agrimi, PhD<sup>5</sup>, Daniela Liccardo, PhD<sup>1,2</sup>, Andrea Elia, PhD<sup>1</sup>, Gizem Keceli, PhD<sup>3</sup>, Giovanna G. Altobelli, MS<sup>4</sup>, Lorenzo Marcucci, PhD<sup>5</sup>, Aram Megighian, MD<sup>5</sup>, Erhe Gao, PhD<sup>2</sup>, Ning Feng, MD, PhD<sup>6</sup>, Kai Kammers, PhD, M Sc.<sup>7</sup>, Nicola Ferrara, MD, PhD<sup>1,4</sup>, Livio Finos, PhD<sup>8</sup>, Walter J. Koch, PhD, FAHA<sup>2,\*\*</sup>, Nazareno Paolucci, MD, PhD<sup>3,5,\*\*</sup>

<sup>1</sup>Department of Translational Medical Science, University of Naples Federico II, Italy;

<sup>2</sup>Center For Translational Medicine LKSOM Temple University, Philadelphia, PA, U.S.A;

<sup>3</sup>Division of Cardiology, Johns Hopkins University Medical Institutions, Baltimore, MD, U.S.A;

<sup>4</sup>Istituti Clinici Scientifici Maugeri - Scientific Institute of Telesse Terme (BN), Italy;

<sup>5</sup>Department of Biomedical Sciences, University of Padova, Padova, Italy;

<sup>6</sup>Division of Cardiology, University of Pittsburgh School of Medicine, Pittsburgh, U.S.A.;

<sup>7</sup>Quantitative Sciences Division – Department of Oncology, Johns Hopkins University School of Medicine, Padova, Italy.

<sup>8</sup>Department of Statistical Science, University of Padova, Padova, Italy.

### Abstract

**Background:** Loss of brain-derived neurotrophic factor (BDNF)/tropomyosin kinase receptor B (TrkB) signaling accounts for brain and cardiac disorders. In neurons, β-adrenergic receptor (βAR) stimulation enhances local BDNF expression. It is unclear if this occurs in a pathophysiological relevant manner in the heart, especially in the βAR-desensitized post-ischemic myocardium. Nor is it fully understood whether and how TrkB agonists counter chronic post-ischemic left ventricle (LV) decompensation, a significant unmet clinical milestone.

**Methods:** We conducted *in vitro* studies using neonatal rat and adult murine cardiomyocytes (CMs), SH-SY5Y neuronal cells, and umbilical vein endothelial cells. We assessed myocardial ischemia (MI) impact in WT, β3AR KO, or myocyte-selective BDNF KO (myoBDNF KO) mice *in vivo* (via coronary ligation (MI) or in isolated hearts with global ischemia-reperfusion (I/R).

\*\*Address correspondence to: **Walter J. Koch, PhD, FAHA**, W.W. Smith Chair in Cardiovascular Medicine, Department of Cardiovascular Sciences, Center for Translational Medicine, Lewis Katz School of Medicine, Temple University, 3500 N. Broad Street, MERB 941, Philadelphia, PA 19140, Tel: 215-707-9820, Fax: 215-707-9890, walter.koch@temple.edu; **Nazareno Paolucci, MD, PhD**, Division of Cardiology, Johns Hopkins University Medical Institutions, Traylor 911, 720 Rutland Avenue, Baltimore, MD, Tel: 410-502-5743, Fax: 410-367-2225, npaoloc1@jhmi.edu.

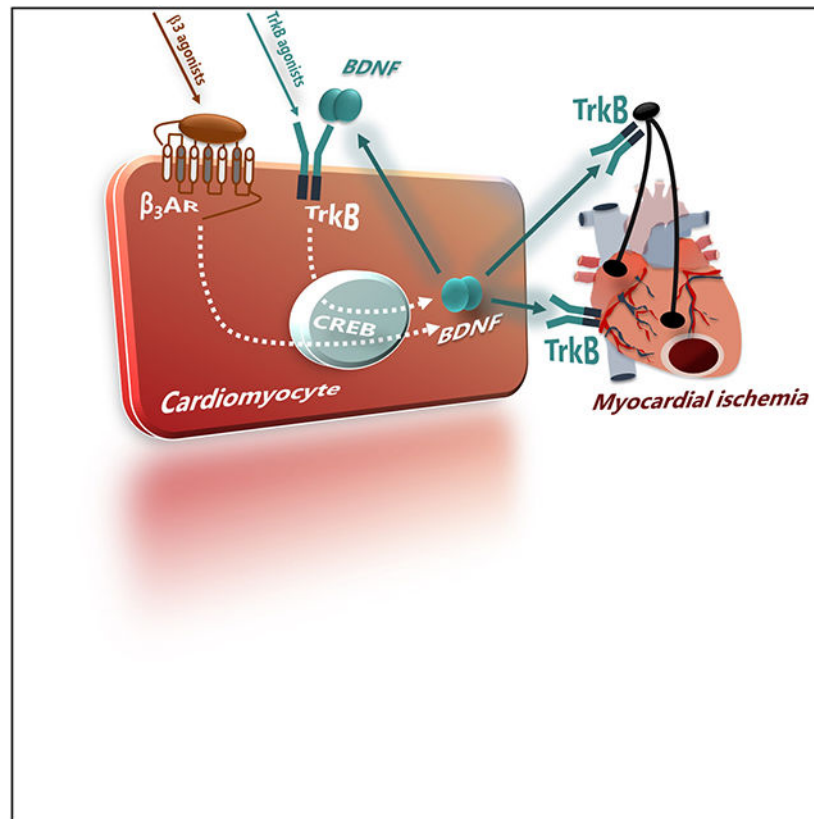
\*These authors equally contributed

Disclosure  
None

**Results:** In WT hearts, BDNF levels rose early after MI (<24 hours), plummeting at four weeks when LV dysfunction, adrenergic denervation, and impaired angiogenesis ensued. The TrkB agonist, LM22A-4, countered all these adverse effects. Compared to WT, isolated myoBDNF KO hearts displayed worse infarct size/LV dysfunction after I/R injury and modest benefits from LM22A-4. *In vitro*, LM22A-4 promoted neurite outgrowth and neovascularization, boosting myocyte function, effects reproduced by 7,8-dihydroxyflavone, a chemically-unrelated TrkB agonist. Superfusing myocytes with the  $\beta$ 3AR-agonist, BRL-37344, increased myocyte BDNF content, while  $\beta$ 3AR signaling underscored BDNF generation/protection in post-MI hearts. Accordingly, the  $\beta$ 1AR blocker, metoprolol, via upregulated  $\beta$ 3ARs, improved chronic post-MI LV dysfunction, enriching the myocardium with BDNF. Lastly, BRL-37344-imparted benefits were nearly abolished in isolated I/R injured myoBDNF KO hearts.

**Conclusions:** BDNF loss underscores chronic post-ischemic heart failure (HF). TrkB agonists can improve ischemic LV dysfunction via replenished myocardial BDNF content. Direct cardiac  $\beta$ 3AR stimulation, or  $\beta$ -blockers (via upregulated  $\beta$ 3AR), is another BDNF-based means to fend off chronic post-ischemic HF.

### Graphical Abstract



### Keywords

Myocardial ischemia; heart failure; BDNF; TrkB;  $\beta$ -AR signaling

**Subject Terms:**

Basic Science Research; Cell Signaling/Signal Transduction; Ischemia; Myocardial Biology; Pathophysiology

---

**INTRODUCTION**

Early mortality after myocardial infarction (MI) declined in the last decades<sup>1</sup>. Yet long-term mortality remains disappointingly high due to chronic heart failure (CHF)<sup>1</sup>, and limiting early post-MI myocyte dropout is paramount to counter it effectively.

In neurons, BDNF and TrkB promote cell growth, connectivity, and stress response<sup>2</sup>. BDNF/TrkB signaling is essential for proper heart development<sup>3</sup>. In adult life, deleting cardiac TrkB impairs basal myocardial contractility/relaxation<sup>4,5</sup>. Conversely, reports on ischemic cardiomyopathy have not unanimously assigned a protective function to BDNF<sup>6-8</sup>. Furthermore, attention has been paid mainly to early post-MI-induced changes in BDNF expression. For instance, *bdnf* mRNA levels double in the ischemic area after MI, correlating with preserved sensory nerve function, but plummet to baseline levels within a few hours<sup>9</sup>. Consistently, elevated early post-MI BDNF improves cardiac function and cardiomyocyte survival<sup>10</sup>. Yet, whether lower cardiac BDNF accounts for CHF pathogenesis is unknown. Likewise, if TrkB stimulation (by mimicking endogenous BDNF actions) arrests CHF progression remains undefined. Nor is it clear whether TrkB signaling is the only route enriching myocardial BDNF content.

Adrenergic receptor (AR) signaling induces BDNF in neurons<sup>11</sup>, particularly  $\beta$ 3AR stimulation<sup>12</sup>. Since in CHF the  $\beta$ AR system is downsized, cardiac BDNF generation should decline during CHF, contributing to its progression. BDNF exerts paracrine salutary actions in neurons, preserving neighboring cells, i.e., endothelial and neuronal cells. Hence, reduced myocardial BDNF pools could also explain sympathetic denervation/impaired angiogenesis in CHF<sup>13-15</sup>. Accordingly, reduced cardiac vascularity worsens post-ischemic myocyte loss<sup>13</sup>, while exacerbated denervation leads to arrhythmias and, ultimately, sudden cardiac death<sup>16</sup>. Hence, measures apt to maintain  $\beta$ AR sensitivity or upregulate  $\beta$ 3ARs expression/activity should implement cardiac BDNF content, thus improving CHF outcomes.

Here, first, we used WT mice to test whether BDNF protein expression changes during post-ischemic CHF, contributing to LV decompensation/remodeling. Second, we interrogated whether and how a TrkB agonist (LM22A-4), beneficial in experimental neurological disorders<sup>17,18</sup>, would attenuate CHF progression in ischemic mice. Third, we tested LM22A-4's impact on neuronal growth, endothelial cells (ECs) proliferation, and cardiomyocyte function *in vitro*. Fourth, we tested its impact in WT MI mice *in vivo*, assessing innervation, angiogenesis, and myocardial function. Fifth, we subjected WT and myocyte-specific *bdnf* knockout (myoBDNF KO) mice to global ischemia/reperfusion (I/R) in the Langendorff to determine myocardial BDNF contribution to post-MI salvage, alone or after TrkB stimulation. Finally,  $\beta$ 3AR stimulation enriches BDNF content in cells<sup>12</sup>. Hence, we interrogated whether TrkB agonist anti-ischemic actions partially depend on  $\beta$ 3AR signaling. We used neonatal rat ventricular myocytes (NRVMs) to assess whether the

$\beta$ 3AR agonist, BRL-37344 enhances myocyte BDNF generation. Then, we tested if  $\beta$ 3AR KO mice bear lower BDNF levels before and after *in vivo* MI. Finally, we administered BRL-37344, known to protect against I/R injury, to myoBDNF KO mice.

## METHODS

Detailed methods are in the Supplemental Material.

Data Availability.

## RESULTS

### Cardiac BDNF expression is reduced in post-ischemic CHF along with impaired angiogenesis and sympathetic innervation

BDNF's role in the pathogenesis of chronic post-ischemic LV decompensation, a significant clinical challenge still<sup>19</sup>, remains unclear. Therefore, *in vivo*, we subjected nine-week-old C57Bl/6 WT mice to MI via permanent coronary artery ligation<sup>20</sup>, using sham-operated animals as controls.

Cardiac BDNF protein abundance was assessed by immunoblot at 6 hours, 24 hours, one week, and four weeks post-MI. BDNF content was elevated 24 hours after MI (Figure 1B). Conversely, it was sizably reduced four weeks after MI (Figure 1C), coincident with chronic post-MI LV decompensation (Figure 1E–F), enlarged LV dimensions (Figure 1G), and elevated fibrotic tissue deposition (Figure 1H). Infarcted hearts displayed a marked drop in capillary density in the remote and border zone compared to shams (Figure 1I). Finally, using tyrosine hydroxylase-positive (TH<sup>+</sup>) nerve fibers as an index of sympathetic nerve fiber density<sup>21</sup>, as expected<sup>16</sup>, we found a drop in cardiac sympathetic innervation (Figure 1J–K). Thus, marked depletion of cardiac BDNF content in the ischemic myocardium parallels cardiac hypo-innervation/reduced capillary density, contributing to post-ischemic CHF pathogenesis.

### TrkB stimulation boosts *in vitro* neuronal sprouting, endothelial cell proliferation, and myocyte function

Next, we interrogated whether the TrkB agonist, LM22A-4, would directly stimulate neuronal sprouting, endothelial cell proliferation, and isolated myocyte function.

**Neuronal cells.**—As shown before<sup>22</sup>, stimulating SH-SY5Y neuronal cells with 100 nM LM22A-4 (for 10 min), a TrkB agonist that, differently from the native BDNF peptide, has a long *in vivo* half-life<sup>17</sup> induced a time-dependent, robust increase in mitogen-activated protein kinase (MAPK) ERK1/2, confirming TrkB receptor activation<sup>17</sup>(Figure 2A). Next, we stimulated these cells with LM22A-4 for 12 hours. This intervention increased the growth-associated protein 43 (GAP43), ultimately enhancing neuronal sprouting (Figure 2B–C).

**Endothelial cells.**—We tested the TrkB agonist impact on human umbilical vein endothelial cells (HUVECs). Compared to vehicle-treated cells, stimulating HUVEC cells

with LM22A-4 for 15 min increased ERK activation (Figure 2D) and Akt and eNOS (Figure 2D–E–F). Adding LM22A-4 for 24 hours to HUVEC cells made endothelial cells proliferate, as witnessed by the BrdU staining results (Figure 2G).

**LV myocytes.**—We isolated adult ventricular myocytes from WT mice (Figure 3A) and conducted a vis-à-vis comparison between LM22A-4, a partial TrkB agonist<sup>23</sup>, and 7,8-dihydroxyflavone (7,8-DHF), a TrkB agonist chemically unrelated to LM22A-4 known to protect against I/R injury<sup>24</sup>. These agents dose-dependently and similarly increased sarcomere shortening and whole Ca<sup>2+</sup> transient (Figure 3B–E and Figure S1). Similarly, they increased ERK phosphorylation to the same extent (Figure 3F). Finally, we tested whether the cotreatment of NVRMs with ANA12, a TrkB antagonist<sup>25</sup>, would abolish the LM22A-4 effect. ANA12 prevented LM22A-4-induced ERK and TrkB phosphorylation (Figure 3G–H). Thus, TrkB stimulation can foster neuronal sprouting and EC proliferation via an Akt/eNOS-dependent signaling switch-on, and sarcolemmal TrkB stimulation can enhance myocyte function, regardless of the agonist used.

### Systemic infusion of the TrkB agonist, LM22A-4 arrests post-ischemic CHF progression

Then, we determined whether TrkB agonism would limit infarct size and LV dysfunction in a relevant preclinical MI model (Figure 4A and Figure S2). First, we infused LM22A-4 (or vehicle = saline) at a rate of 0.2 mg/kg/day (dose molded on previous studies in the brain<sup>17</sup>) into WT sham-operated mice. This agent did not alter basal myocardial performance (Table S1). Next, we administered it to WT mice, using sham-operated animals and vehicle-treated MI mice as controls. One week after MI, we randomized the mice to placebo or LM22A-4 treatment (Figure S2). Four weeks post-MI, mice treated with LM22A-4 had significantly mitigated infarct size than control MI mice (Figure 4B), with substantially preserved LV function (Figure 2C) and attenuated LV adverse remodeling (Figure 2D–E), in the absence of a sizable impact on heart rate (HR) (Figure S3). MI led to prominent collagen deposition in vehicle-treated mice, an effect mitigated sizably by LM22A-4 (Figure 4F). This treatment also rescued vessel density (in the remote and border zone) and maintained myocardial sympathetic innervation (Figure 4G–H). After LM22A4 treatment, post-MI hearts were markedly enriched in BDNF content (Figure 4I). Finally, as shown in Figure S4, Akt-phosphorylation levels increased in MI hearts. Still, they returned to baseline values after LM22A-4, in keeping with the idea that chronically elevated Akt activity underpins adverse remodeling and loss of inotropy<sup>26</sup>. Thus, TrkB agonism arrests CHF progression via BDNF-evoked improvement of myocardial cell survival/function and preserved cardiac sympathetic innervation and vascularity.

### Stimulating cardiac TrkB limits I/R injury in isolated WT but not myoBDNF KO hearts

TrkB stimulation induces a battery of pro-survival genes in neurons, including *bdnf* itself<sup>27</sup>, via CREB-mediated signaling<sup>28</sup>. Hence, we tested whether TrkB stimulation benefits require myocyte BDNF generation besides neuronal effects. We subjected WT and myoBDNF KO (Figure 5A) to 30 min global ischemia/2hrs reperfusion in the Langendorff, with or without the TrkB agonist, LM22A-4 (20 μM for 10 minutes following ischemia), or vehicle (perfusion buffer). LM22A-4 given to WT hearts at reperfusion substantially reduced infarct size (Figure 5B–C) while improving post-ischemic LV function. When subjected to I/R

injury, myoBDNF KO hearts showed exacerbated myocyte loss (Figure 5C–D) and LV dysfunction than WT hearts (Figure 5E, G–I). Of note, changes in heart rate (HR) (Figure 5F) did not contribute to the different rate-pressure products (RPP) observed after LM22A-4 treatment in both genotypes at reperfusion. Of note, 12–16 weeks-old WT and myoBDNF KO mice have similar basal LV functions (Figure 5; Figure S5/Table S2) and significantly abated BDNF content/expression (Figure S6C–D). Finally, the TUNEL assay<sup>29</sup> showed higher TUNEL-positive myocytes in myoBDNF KO than WT (Figure 5J). Thus, lack of myocyte BDNF is associated with worse outcomes after I/R injury.

### **β3AR-stimulation increases BDNF production in isolated myocytes, and β3AR signaling accounts for BDNF generation in post-ischemic hearts**

In hippocampal neurons, norepinephrine (Nepi) induces BDNF<sup>11</sup>. Nepi-induced BDNF generation in some tumors leads to expanded β3AR-dependent intratumoral innervation<sup>12</sup>. Thus, we determined whether selective β3AR stimulation boosts autologous BDNF myocyte generation. We treated NRVMs with Nepi (10 μM) or the specific β3AR-agonist, BRL-37344 (1 μM). Both stimulants heightened myocyte BDNF expression significantly. However, BRL-37344 was more effective than Nepi (Figure 6A). Then, pre-treating NRVMs with the selective competitive β3AR-blocker, SR58894A, and then stimulating them with Nepi (for 12 hours), we found that SR58894A prevented NEpi- (Figure 6B) and BRL 37344-induced enhanced BDNF expression (Figure 6C). Thus, β3AR activation accounts, at least in part, for NEpi-induced BDNF generation in the heart. We confirmed this eventuality by exposing NRVMs to the β1-blocker metoprolol (Meto; 10 μM, for 30 min) (Figure S7B). Indeed, selective β1-blockers can promote β3AR upregulation in experimental HF settings, accounting for β1-blockade benefits<sup>20,21,27,30</sup>. Moreover, β-blockers improve endothelial function and promote vasorelaxation, an effect for which β3AR activation chiefly accounts<sup>15,27,28</sup>. Therefore, we exposed NRVMs to either NEpi (10 μM) or BRL 37344 (BRL, 1 μM) for 12 hrs. Congruent with data in Figure 6A, NEpi and BRL (each taken alone) heightened BDNF expression in NRVMs (Figure S7B). Of relevance, pre-treating cells with Meto potentiated NEpi's ability to induce BDNF expression (Figure S7B). Thus, by making more catecholamines available to bind to β3ARs, and not to β1ARs, as documented<sup>20</sup>, Meto rescues β3AR-dependent BDNF expression.

Next, MI markedly downregulates β3ARs<sup>20</sup>. Thus, we speculated that lack of β3ARs signaling would depauperate the post-ischemic CHF heart of BDNF. Hence, as done before<sup>20</sup>, one week after MI, mice were assigned (in a random fashion) to 3 weeks of either saline or Meto. Meto prevented cardiac function deterioration occurring four weeks after MI (Figure S7C), preserved BDNF expression (Figure S7D), increased capillary density in the remote zone (compared to MI control mice, Figure S7E), and better maintained TH<sup>+</sup> fiber number (Figure S7F). Thus, chronic β1AR blockade via Meto reignites cardiac β3AR/BDNF signaling in post-ischemic CHF murine hearts.

Next, we evaluated whether BDNF protein abundance changed in WT and β3AR KO-infarcted mice (Figure 6D–E). Sham-operated or infarcted β3AR KO hearts exhibited BDNF and TH protein levels and TH<sup>+</sup> fiber amount superimposable to those found in infarcted WT counterparts (Figure 6F–H). Likewise, vessel density ranks were markedly lower in β3AR



KO sham hearts compared to WT (Figure 6I). After MI, sympathetic fiber density dropped equally in WT and  $\beta$ 3AR KO, although capillary density declined less in  $\beta$ 3AR KO mice (Figure 6G,I). There is a profound  $\beta$ 3AR downregulation after MI<sup>20</sup>. Thus, it is unsurprising that LV dysfunction/remodeling is superimposable in WT and  $\beta$ 3AR KO mice after MI. Moreover, we found that LM22A-4 recovered LV function and reduced infarct size in both genotypes (Figure 6 and S8). However, in  $\beta$ 3AR KO mice, LM22A-afforded protection lasted only one week after MI (Figure S8). Thus, TrkB agonist anti-ischemic actions are partly  $\beta$ 3AR-mediated, therefore, more prominent with preserved  $\beta$ 3AR signaling.

### **$\beta$ 3AR benefits against I/R injury are lost in myoBDNF KO mice**

Finally, we interrogated whether the selective  $\beta$ 3 agonist administration, BRL-37344 prevents I/R in isolated WT murine hearts and if this protection is, at least in part, myocyte BDNF-dependent (Figure 7A). Therefore, we inflicted global I/R injury to WT and myoBDNF KO mice, with or without BRL-37344 (10  $\mu$ M for 10 minutes, starting at reperfusion). As expected, myoBDNF KO mice had larger infarct sizes and exacerbated LV function than WT mice (Figure 7B–H). BRL-37344 protected WT hearts against I/R injury, consistent with recent studies<sup>31</sup>: infarct size was reduced with BRL-37344 (Figure 7B–C), despite no sizable LV function improvement (Figure 7D–H). Of relevance, BRL-37344-granted protection was markedly attenuated in myoBDNF KO animals (Figure 7B–D, F–H): see, for instance, the larger infarct size in myoBDNF KO vs. WT mice (Figure 7B–C). Also, BRL-37344 treatment significantly lowered TUNEL-positive myocytes in WT hearts but not in myoBDNF KO ones (Figure 7I). Thus,  $\beta$ 3-agonist anti-ischemic effects stem partly from myocyte BDNF generation, and altered  $\beta$ 3AR-dependent signaling in the ischemic heart underscores the loss of cardiac BDNF-bestowed autocrine/paracrine beneficial actions (Figure 8).

## **DISCUSSION**

Here we show that: 1) BDNF protein expression is elevated within 24hrs after MI, consistent with previous studies<sup>9</sup> but reduced when CHF ensues (i.e., four weeks after MI), contributing to impaired angiogenesis, innervation, and cardiomyocyte function; 2) TrkB agonists, such as LM22A-4 arrest CHF progression, countering all these adverse effects; 3) preventing or limiting myocyte BDNF generation (via *bdnf* deletion) exacerbates I/R injury while downsizing the benefits afforded by cardiac TrkB stimulation; 4) superfusing cardiomyocytes with a  $\beta$ 3AR agonist enriches myocyte BDNF content while constitutive  $\beta$ 3AR gene deletion curtails BDNF expression *in vivo*; 5)  $\beta$ 3AR agonists protect isolated hearts from global I/R injury, an effect attenuated in myocyte *bdnf*-deleted hearts. Finally, the  $\beta$ -blocker Meto, by upregulating  $\beta$ 3ARs signaling in the post-ischemic heart, improves chronic post-MI LV dysfunction, enriching the myocardium with BDNF.

### **BDNF and $\beta$ AR signaling in CHF**

Autocrine BDNF generation occurs in an organ-specific response in many peripheral organs in response to stress conditions. For instance, the contracting skeletal muscle enhances autologous BDNF production to increase fatty acid oxidation<sup>27</sup>, representing one source of incremented serum BDNF levels after exercise<sup>28</sup>. BDNF is essential in the heart for cardiac

development and function in adulthood<sup>3</sup>. Low levels of BDNF are associated with adverse cardiac remodeling and higher levels of NTproBNP<sup>32</sup>. Moreover, we recently showed that BDNF regulates cardiac bioenergetics by modulating the expression of the transcription factor Yin Yang1<sup>33</sup>.

With overt HF, as in the case of chronic LV dysfunction occurring four weeks after infarcted in mice<sup>20</sup>, the initial compensatory sympathetic overdrive<sup>34,35</sup> becomes maladaptive, altering  $\beta$ ARs sensitivity/coupling to G proteins, ultimately lowering cardiac contractility/inotropic reserve<sup>35</sup>. Among other signatures of adrenergic dysregulation, there is a substantial loss of  $\beta$ 1AR density ( $\approx$ 50%) at the plasma membrane level and a marked dysfunction of  $\beta$ 3AR, too<sup>20,36</sup>. Here, we report, for the first time, that an altered cardiac  $\beta$ AR signaling accounts for reduced autologous myocardial BDNF generation late after MI when CHF ensues.

**Role of  $\beta$ 3AR signaling.**— $\beta$ 3AR signaling is beneficial in several forms of HF<sup>37</sup> including those caused by post-ischemic injury<sup>20,38</sup>. Here, we show that, in NRVMs,  $\beta$ 3AR stimulation via BRL-37344 directly enriches them with BDNF, whereas  $\beta$ 3AR blockade via SR58894A prevents it. Furthermore, altered  $\beta$ 3AR signaling lowers cardiac BDNF content *in vivo*. Indeed, at baseline,  $\beta$ 3AR KO hearts already display sizably lowered BDNF protein abundance, coupled to reduced TH protein/TH<sup>+</sup> fiber content, and capillary density; notably, at levels comparable to found in infarcted WT mice (Figure 6F). Moreover, Meto that upregulates  $\beta$ 3AR expression/activity<sup>20,30</sup> rescues cardiac BDNF content, improving LV dysfunction/remodeling, while favoring neoangiogenesis and sympathetic reinnervation (Figure S7). Thus, defective  $\beta$ 3AR signaling can still underscore worsened post-MI cardiac dysfunction/remodeling, rendering the heart insensitive (or partially responsive) to mainstay anti-HF drugs, such as  $\beta$ 1/ $\beta$ 2 blockers<sup>20</sup> whose protective profile relies, at least partly, upon  $\beta$ 3AR upregulation<sup>39</sup>. Congruently, despite an initial protection (until one week after MI, Figure S8), LM22A-4 benefits disappear four weeks after MI in  $\beta$ 3AR KO mice because BDNF is already limited in this mouse strain.

Not surprisingly, BRL-37344 limited infarct size in I/R injured WT mice but did not improve post-ischemic LV function. Indeed, as reviewed<sup>40</sup>,  $\beta$ 3AR protection could be due to nitric oxide/cGMP signaling that may have antioxidant, metabolic, and/or vasorelaxant actions, but also negative inotropic actions, especially at high concentrations<sup>41</sup>. While  $\beta$ 3AR autoantibodies can exert negative chronotropy/inotropy via decreased intracellular Ca<sup>2+</sup> transient/membrane L-type Ca<sup>2+</sup> currents in cardiomyocytes<sup>42</sup>. Yet, as with  $\beta$ 1 or  $\beta$ 2 constitutive deletion<sup>43,44</sup>, knocking down  $\beta$ 3AR from birth does not affect basal LV function<sup>20</sup>, likely owing to compensatory mechanisms taking over with time. Conditional  $\beta$ 3AR KO mice would be of great help in further dissecting  $\beta$ 3AR-evoked myocyte BDNF generation at different stages after MI.

Here we show, for the first time, that autologous myocyte BDNF production is part of the  $\beta$ 3AR- and Meto-driven protective effects in the post-ischemic heart and provide the first evidence linking a specific  $\beta$ AR subtype to BDNF generation in myocytes.



## TrkB agonists and ischemic cardiomyopathy

BDNF/TrkB activation alleviates cardiac dysfunction, dilation, infarct size, and ischemia-induced apoptosis from ischemia-reperfusion injury<sup>10</sup>. The TrkB agonist 7,8-DHF improves post-ischemic LV dysfunction, inhibiting excessive mitochondrial fission by activating Akt and reducing the proteolytic cleavage of optic atrophy 1 in isolated myocytes challenged with ischemia/H<sub>2</sub>O<sub>2</sub><sup>24</sup>. Here, we demonstrate that chronic LM22A-4 supplementation to MI mice enriches the myocardium with BDNF, thus confirming the existence of a virtuous loop: *circulating BDNF - sarcolemmal TrkB stimulation – myocyte BDNF generation* – whereby cardiac TrkB stimulation turns on pro-survival genes, including *bdnf* itself. This scenario conforms to what is found in neurons<sup>45</sup>, where BDNF/TrkB signaling regulates neurite outgrowth/synaptogenesis<sup>46</sup> in an autocrine/paracrine fashion<sup>47</sup>. The post-ischemic heart is sympathetically denervated<sup>48</sup> and catecholamine-depleted<sup>49</sup>, thus explaining its progression to CHF. Current chronic administration of LM22A-4 rescued sympathetic innervation and capillary density to baseline levels while attenuating fibrotic tissue deposition. The latter evidence suggests attenuated myocyte loss, and our present data in infarcted WT hearts confirmed LM22A-4's ability to counter apoptosis<sup>50</sup>. Furthermore, two chemically-unrelated TrkB agonists enhance sarcomere shortening/whole Ca<sup>2+</sup> transient similarly while triggering ERK phosphorylation. Hence, TrkB agonists fully mimic the effects of exogenous (recombinant) BDNF applied to isolated murine myocytes<sup>4</sup> or hearts<sup>51</sup>. Finally, myoBDNF KO hearts displayed worse outcomes than WT after global I/R injury in isolated hearts (thus minimizing confounding neurohormonal effects). The present evidence dovetails nicely with the “*neurotrophin hypothesis*”: only those neurons synthesizing (or retaining) enough neurotrophins would survive during development and under stress conditions in adulthood<sup>11</sup>. Accordingly, TrkB agonist protection is markedly blunted in myoBDNF KO mice, again validating that, by binding to sarcolemmal TrkB, exogenous BDNF triggers a virtuous loop involving myocyte BDNF content rise. When long applied, the TrkB agonist would stimulate CREB to induce pro-survival gene expression, including *bdnf* itself<sup>51</sup>. When administered for a short time, it may prompt a more rapid conversion of pre-constituted proBDNF into mature BDNF, an intriguing possibility that remains to be tested.

## Limitations and Studies in Perspective

First, we focused on four weeks after MI, when chronic post-MI LV decompensation begins manifesting in mice<sup>20</sup>. Second, BDNF regulates HR by mechanisms involving augmented brainstem parasympathetic neuron excitability<sup>52</sup>. Vagal control of myocardial function is altered in HF<sup>53</sup>. Hence, like endogenous BDNF that increases acetylcholine release from autonomic neurons and lowers cardiac myocyte beat frequency<sup>52</sup>, TrkB agonists may promote a more balanced sympathetic/parasympathetic reinnervation/function in CHF. And the unchanged HR after chronic TrkB agonist supplementation is highly suggestive of this possibility. Third, BDNF/TrkB stimulation enhances survival in neurons through several highly intermingled signaling pathways, including PI3K, ERK, and CaMK, all ultimately impinging on CREB signaling<sup>51,54</sup>. ERK activation subtends the pro-proliferative and inotropic action of TrkB agonists in neuronal, endothelial cells, and cardiomyocytes. However, a more nuanced dissection of BDNF/TrkB-evoked pro-survival pathways in the post-ischemic myocardium is warranted. Finally, LM22A-4 positive inotropy is attenuated in Langendorff I/R injured hearts (Figure 5), apparently at odds with the TrkB agonist-

induced enhancement of isolated cardiomyocyte function (Figure 3). Yet, this evidence could be part of the well-known phenomenon of myocardial stunning, i.e., reversible loss of contractile activity occurring despite the restoration of adequate blood flow, *ex-vivo*<sup>55</sup> and *in vivo*<sup>56</sup>. This eventuality remains to be tested. How the TrkB/ $\beta$ 3AR interaction benefits post-ischemic CHF remains to be deciphered in full, keeping enhanced metabolism<sup>57</sup> and/or enduring anti-apoptotic effects<sup>58</sup> in the bull's eye.

## CONCLUSION

When impaired, the BDNF/TrkB system contributes to post-ischemic CHF pathogenesis. TrkB agonists attenuates CHF progression by offsetting the loss of myocyte, sympathetic fibers, and capillaries. Chronic TrkB stimulation in mice with I/R injury enriches the myocardium with autologous BDNF, thus limiting these losses while rescuing LV function.  $\beta$ 3AR is another previously unrecognized route leading to myocyte BDNF production. This evidence explains, at least partially, why  $\beta$ 1-blockers, such as Meto, protect the ischemic myocardium, i.e., via enhanced  $\beta$ AR3-driven BDNF generation.

Our study expands the portfolio of the heart's compensatory systems and cardio-endocrine capacities against ischemic and (possibly) non-ischemic stress conditions. We propose a virtuous loop - *cardiac TrkB-stimulation due to extrinsic BDNF to induce myocardial-intrinsic BDNF production* – as a new means to limit ischemic injury. Alone or with other anti-HF therapies, TrkB agonists could arrest post-ischemic CHF through the benefits of autocrine and paracrine BDNF.

## Supplementary Material

Refer to Web version on PubMed Central for supplementary material.

## Acknowledgments

We are very thankful to Drs. Mark P. Mattson and Robert G. Weiss (JHU) for their critical manuscript reading and suggestions.

## Source of Fundings

The present work was supported by: NIH grants R37 HL061690, R01 HL088503, P01 HL08806, P01 HL075443, P01 HK091799 (to WJK), and R01 HL136918 (to N.P.) and R01 HL063030 (to NP as co-PI). GK is supported by funds from the Johns Hopkins University Older American Independence Center of the National Institute on Aging (NIA) under award number P30AG021334.

## Data availability

The data supporting this study's findings, including statistical analyses and reagents used, are available from the corresponding author upon request.

## Nonstandard Abbreviations and Acronyms:

$\beta$ AR	$\beta$ -adrenergic receptor
BDNF	brain-derived neurotrophic factor

<b>CHF</b>	chronic heart failure
<b>GAP43</b>	growth-associated protein 43
<b>HF</b>	heart failure
<b>HUVEC</b>	human umbilical vein endothelial cell
<b>LV</b>	left ventricle
<b>MAPK</b>	mitogen-activated protein kinase
<b>MI</b>	myocardial ischemia
<b>NRVM</b>	neonatal rat ventricular myocyte
<b>TrkB</b>	tropomyosin kinase receptor B

## REFERENCES

- Johansson S, Rosengren A, Young K, Jennings E. Mortality and morbidity trends after the first year in survivors of acute myocardial infarction: a systematic review. *BMC Cardiovasc Disord.* 2017;17:53. doi: 10.1186/s12872-017-0482-9 [PubMed: 28173750]
- Benarroch EE. Brain-derived neurotrophic factor: Regulation, effects, and potential clinical relevance. *Neurology.* 2015;84:1693–1704. doi: 10.1212/WNL.0000000000001507 [PubMed: 25817841]
- Kermani P, Hempstead B. BDNF Actions in the Cardiovascular System: Roles in Development, Adulthood and Response to Injury. *Front Physiol.* 2019;10:455. doi: 10.3389/fphys.2019.00455 [PubMed: 31105581]
- Feng N, Huke S, Zhu G, Tocchetti CG, Shi S, Aiba T, Kaludercic N, Hoover DB, Beck SE, Mankowski JL, et al. Constitutive BDNF/TrkB signaling is required for normal cardiac contraction and relaxation. *Proc Natl Acad Sci U S A.* 2015;112:1880–1885. doi: 10.1073/pnas.1417949112 [PubMed: 25583515]
- Fulgenzi G, Tomassoni-Ardori F, Babini L, Becker J, Barrick C, Puverel S, Tessarollo L. BDNF modulates heart contraction force and long-term homeostasis through truncated TrkB.T1 receptor activation. *J Cell Biol.* 2015;210:1003–1012. doi: 10.1083/jcb.201502100 [PubMed: 26347138]
- Halade GV, Ma Y, Ramirez TA, Zhang J, Dai Q, Hensler JG, Lopez EF, Ghasemi O, Jin YF, Lindsey ML. Reduced BDNF attenuates inflammation and angiogenesis to improve survival and cardiac function following myocardial infarction in mice. *Am J Physiol Heart Circ Physiol.* 2013;305:H1830–1842. doi: 10.1152/ajpheart.00224.2013 [PubMed: 24142413]
- Katara RG, Kakinuma Y, Arikawa M, Yamasaki F, Sato T. Chronic intermittent fasting improves the survival following large myocardial ischemia by activation of BDNF/VEGF/PI3K signaling pathway. *J Mol Cell Cardiol.* 2009;46:405–412. doi: 10.1016/j.yjmcc.2008.10.027 [PubMed: 19059263]
- Okada S, Yokoyama M, Toko H, Tateno K, Moriya J, Shimizu I, Nojima A, Ito T, Yoshida Y, Kobayashi Y, et al. Brain-derived neurotrophic factor protects against cardiac dysfunction after myocardial infarction via a central nervous system-mediated pathway. *Arterioscler Thromb Vasc Biol.* 2012;32:1902–1909. doi: 10.1161/ATVBAHA.112.248930 [PubMed: 22556331]
- Hiltunen JO, Laurikainen A, Vakeva A, Meri S, Saarna M. Nerve growth factor and brain-derived neurotrophic factor mRNAs are regulated in distinct cell populations of rat heart after ischaemia and reperfusion. *J Pathol.* 2001;194:247–253. doi: 10.1002/path.878 [PubMed: 11400155]
- Hang P, Zhao J, Cai B, Tian S, Huang W, Guo J, Sun C, Li Y, Du Z. Brain-derived neurotrophic factor regulates TRPC3/6 channels and protects against myocardial infarction in rodents. *Int J Biol Sci.* 2015;11:536–545. doi: 10.7150/ijbs.10754 [PubMed: 25892961]

11. Chen MJ, Nguyen TV, Pike CJ, Russo-Neustadt AA. Norepinephrine induces BDNF and activates the PI-3K and MAPK cascades in embryonic hippocampal neurons. *Cell Signal*. 2007;19:114–128. doi: 10.1016/j.cellsig.2006.05.028 [PubMed: 16876982]
12. Allen JK, Armaiz-Pena GN, Nagaraja AS, Sadaoui NC, Ortiz T, Dood R, Ozcan M, Herder DM, Haemmerle M, Gharpure KM, et al. Sustained Adrenergic Signaling Promotes Intratumoral Innervation through BDNF Induction. *Cancer Res*. 2018;78:3233–3242. doi: 10.1158/0008-5472.CAN-16-1701 [PubMed: 29661830]
13. Shiojima I, Sato K, Izumiya Y, Schiekofe S, Ito M, Liao R, Colucci WS, Walsh K. Disruption of coordinated cardiac hypertrophy and angiogenesis contributes to the transition to heart failure. *J Clin Invest*. 2005;115:2108–2118. doi: 10.1172/JCI24682 [PubMed: 16075055]
14. Jacobson AF, Senior R, Cerqueira MD, Wong ND, Thomas GS, Lopez VA, Agostini D, Weiland F, Chandna H, Narula J, et al. Myocardial iodine-123 meta-iodobenzylguanidine imaging and cardiac events in heart failure. Results of the prospective ADMIRE-HF (AdreView Myocardial Imaging for Risk Evaluation in Heart Failure) study. *J Am Coll Cardiol*. 2010;55:2212–2221. doi: 10.1016/j.jacc.2010.01.014 [PubMed: 20188504]
15. Rengo G, Cannavo A, Liccardo D, Zincarelli C, de Lucia C, Pagano G, Komici K, Parisi V, Scala O, Agresta A, et al. Vascular endothelial growth factor blockade prevents the beneficial effects of beta-blocker therapy on cardiac function, angiogenesis, and remodeling in heart failure. *Circ Heart Fail*. 2013;6:1259–1267. doi: 10.1161/CIRCHEARTFAILURE.113.000329 [PubMed: 24029661]
16. Fukuda K, Kanazawa H, Aizawa Y, Ardell JL, Shivkumar K. Cardiac innervation and sudden cardiac death. *Circ Res*. 2015;116:2005–2019. doi: 10.1161/CIRCRESAHA.116.304679 [PubMed: 26044253]
17. Massa SM, Yang T, Xie Y, Shi J, Bilgen M, Joyce JN, Nehama D, Rajadas J, Longo FM. Small molecule BDNF mimetics activate TrkB signaling and prevent neuronal degeneration in rodents. *J Clin Invest*. 2010;120:1774–1785. doi: 10.1172/JCI41356 [PubMed: 20407211]
18. Zeng Y, Wang X, Wang Q, Liu S, Hu X, McClintock SM. Small molecules activating TrkB receptor for treating a variety of CNS disorders. *CNS Neurol Disord Drug Targets*. 2013;12:1066–1077. doi: 10.2174/18715273113129990089 [PubMed: 23844685]
19. Keceli G, Majumdar A, Thorpe CN, Jun S, Tocchetti CG, Lee DI, Mahaney JE, Paolucci N, Toscano JP. Nitroxyl (HNO) targets phospholamban cysteines 41 and 46 to enhance cardiac function. *J Gen Physiol*. 2019;151:758–770. doi: 10.1085/jgp.201812208 [PubMed: 30842219]
20. Cannavo A, Rengo G, Liccardo D, Pun A, Gao E, George AJ, Gambino G, Rapacciuolo A, Leosco D, Ibanez B, et al. beta1-Blockade Prevents Post-Ischemic Myocardial Decompensation Via beta3AR-Dependent Protective Sphingosine-1 Phosphate Signaling. *J Am Coll Cardiol*. 2017;70:182–192. doi: 10.1016/j.jacc.2017.05.020 [PubMed: 28683966]
21. Rasmussen P, Brassard P, Adser H, Pedersen MV, Leick L, Hart E, Secher NH, Pedersen BK, Pilegaard H. Evidence for a release of brain-derived neurotrophic factor from the brain during exercise. *Exp Physiol*. 2009;94:1062–1069. doi: 10.1113/expphysiol.2009.048512 [PubMed: 19666694]
22. Nguyen HTH, Wood RJ, Prawdiuk AR, Furness SGB, Xiao J, Murray SS, Fletcher JL. TrkB Agonist LM22A-4 Increases Oligodendroglial Populations During Myelin Repair in the Corpus Callosum. *Front Mol Neurosci*. 2019;12:205. doi: 10.3389/fnmol.2019.00205 [PubMed: 31507374]
23. Fletcher JL, Dill LK, Wood RJ, Wang S, Robertson K, Murray SS, Zamani A, Semple BD. Acute treatment with TrkB agonist LM22A-4 confers neuroprotection and preserves myelin integrity in a mouse model of pediatric traumatic brain injury. *Exp Neurol*. 2021;339:113652. doi: 10.1016/j.expneurol.2021.113652 [PubMed: 33609501]
24. Wang Z, Wang SP, Shao Q, Li PF, Sun Y, Luo LZ, Yan XQ, Fan ZY, Hu J, Zhao J, et al. Brain-derived neurotrophic factor mimetic, 7,8-dihydroxyflavone, protects against myocardial ischemia by rebalancing optic atrophy 1 processing. *Free Radic Biol Med*. 2019;145:187–197. doi: 10.1016/j.freeradbiomed.2019.09.033 [PubMed: 31574344]
25. Cazorla M, Premont J, Mann A, Girard N, Kellendonk C, Rognan D. Identification of a low-molecular weight TrkB antagonist with anxiolytic and antidepressant activity in mice. *J Clin Invest*. 2011;121:1846–1857. doi: 10.1172/JCI43992 [PubMed: 21505263]

26. Walkowski B, Kleibert M, Majka M, Wojciechowska M. Insight into the Role of the PI3K/Akt Pathway in Ischemic Injury and Post-Infarct Left Ventricular Remodeling in Normal and Diabetic Heart. *Cells*. 2022;11. doi: 10.3390/cells11091553
27. Matthews VB, Astrom MB, Chan MH, Bruce CR, Krabbe KS, Prelovsek O, Akerstrom T, Yfanti C, Broholm C, Mortensen OH, et al. Brain-derived neurotrophic factor is produced by skeletal muscle cells in response to contraction and enhances fat oxidation via activation of AMP-activated protein kinase. *Diabetologia*. 2009;52:1409–1418. doi: 10.1007/s00125-009-1364-1 [PubMed: 19387610]
28. Walsh JJ, Tschakovsky ME. Exercise and circulating BDNF: Mechanisms of release and implications for the design of exercise interventions. *Appl Physiol Nutr Metab*. 2018;43:1095–1104. doi: 10.1139/apnm-2018-0192 [PubMed: 29775542]
29. Agrimi J, Scalco A, Agafonova J, Williams Iii L, Pansari N, Keceli G, Jun S, Wang N, Mastorci F, Tichnell C, et al. Psychosocial Stress Hastens Disease Progression and Sudden Death in Mice with Arrhythmogenic Cardiomyopathy. *J Clin Med*. 2020;9. doi: 10.3390/jcm9123804
30. Trapanese DM, Liu Y, McCormick RC, Cannavo A, Nanayakkara G, Baskharoun MM, Jarrett H, Woitek FJ, Tillson DM, Dillon AR, et al. Chronic beta1-adrenergic blockade enhances myocardial beta3-adrenergic coupling with nitric oxide-cGMP signaling in a canine model of chronic volume overload: new insight into mechanisms of cardiac benefit with selective beta1-blocker therapy. *Basic Res Cardiol*. 2015;110:456. doi: 10.1007/s00395-014-0456-3 [PubMed: 25480109]
31. Salie R, Alsalhin AKH, Marais E, Lochner A. Cardioprotective Effects of Beta3-Adrenergic Receptor (beta3-AR) Pre-, Per-, and Post-treatment in Ischemia-Reperfusion. *Cardiovasc Drugs Ther*. 2019;33:163–177. doi: 10.1007/s10557-019-06861-5 [PubMed: 30729348]
32. Bahls M, Konemann S, Markus MRP, Wenzel K, Friedrich N, Nauck M, Volzke H, Steveling A, Janowitz D, Grabe HJ, et al. Brain-derived neurotrophic factor is related with adverse cardiac remodeling and high NTproBNP. *Sci Rep*. 2019;9:15421. doi: 10.1038/s41598-019-51776-8 [PubMed: 31659205]
33. Yang X, Zhang M, Xie B, Peng Z, Manning JR, Zimmerman R, Wang Q, Wei AC, Khalifa M, Reynolds M, et al. Myocardial brain-derived neurotrophic factor regulates cardiac bioenergetics through the transcription factor Yin Yang 1. *Cardiovasc Res*. 2022. doi: 10.1093/cvr/cvac096
34. Cannavo A, Liccardo D, Lymperopoulos A, Santangelo M, Femminella GD, Leosco D, Cittadini A, Ferrara N, Paolucci N, Koch WJ, et al. GRK2 Regulates alpha2-Adrenergic Receptor-Dependent Catecholamine Release in Human Adrenal Chromaffin Cells. *J Am Coll Cardiol*. 2017;69:1515–1517. doi: 10.1016/j.jacc.2017.01.016 [PubMed: 28302297]
35. Bristow MR, Ginsburg R, Minobe W, Cubicciotti RS, Sageman WS, Lurie K, Billingham ME, Harrison DC, Stinson EB. Decreased catecholamine sensitivity and beta-adrenergic-receptor density in failing human hearts. *N Engl J Med*. 1982;307:205–211. doi: 10.1056/NEJM198207223070401 [PubMed: 6283349]
36. Zhang Z, Ding L, Jin Z, Gao G, Li H, Zhang L, Zhang L, Lu X, Hu L, Lu B, et al. Nebivolol protects against myocardial infarction injury via stimulation of beta 3-adrenergic receptors and nitric oxide signaling. *PLoS One*. 2014;9:e98179. doi: 10.1371/journal.pone.0098179 [PubMed: 24849208]
37. Pun-García A, Clemente-Moragón A, Villena-Gutierrez R, Gómez M, Sanz-Rosa D, Díaz-Guerra A, Prados B, Medina JP, Montó F, Ivorra MD et al. Beta-3 adrenergic receptor overexpression reverses aortic stenosis-induced heart failure and restores balanced mitochondrial dynamics. *Basic Res Cardiol*. 2022;117:62. doi: 10.1007/s00395-022-00966-z [PubMed: 36445563]
38. Garcia-Prieto J, Garcia-Ruiz JM, Sanz-Rosa D, Pun A, Garcia-Alvarez A, Davidson SM, Fernandez-Friera L, Nuno-Ayala M, Fernandez-Jimenez R, Bernal JA, et al. beta3 adrenergic receptor selective stimulation during ischemia/reperfusion improves cardiac function in translational models through inhibition of mPTP opening in cardiomyocytes. *Basic Res Cardiol*. 2014;109:422. doi: 10.1007/s00395-014-0422-0 [PubMed: 24951958]
39. Michel LYM, Farah C, Balligand JL. The Beta3 Adrenergic Receptor in Healthy and Pathological Cardiovascular Tissues. *Cells*. 2020;9. doi: 10.3390/cells9122584 [PubMed: 33375150]
40. Balligand JL. Cardiac salvage by tweaking with beta-3-adrenergic receptors. *Cardiovasc Res*. 2016;111:128–133. doi: 10.1093/cvr/cvw056 [PubMed: 27001422]

41. Cannavo A, Koch WJ. Targeting beta3-Adrenergic Receptors in the Heart: Selective Agonism and beta-Blockade. *J Cardiovasc Pharmacol.* 2017;69:71–78. doi: 10.1097/FJC.0000000000000444 [PubMed: 28170359]
42. Wang J, Li M, Ma X, Bai K, Wang L, Yan Z, Lv T, Zhao Z, Zhao R, Liu H. Autoantibodies against the beta3-adrenoceptor protect from cardiac dysfunction in a rat model of pressure overload. *PLoS One.* 2013;8:e78207. doi: 10.1371/journal.pone.0078207 [PubMed: 24147120]
43. Rohrer DK, Desai KH, Jasper JR, Stevens ME, Regula DP Jr., Barsh GS, Bernstein D, Kobilka BK. Targeted disruption of the mouse beta1-adrenergic receptor gene: developmental and cardiovascular effects. *Proc Natl Acad Sci U S A.* 1996;93:7375–7380. doi: 10.1073/pnas.93.14.7375 [PubMed: 8693001]
44. Chruscinski AJ, Rohrer DK, Schauble E, Desai KH, Bernstein D, Kobilka BK. Targeted disruption of the beta2 adrenergic receptor gene. *J Biol Chem.* 1999;274:16694–16700. doi: 10.1074/jbc.274.24.16694 [PubMed: 10358008]
45. Camandola S, Mattson MP. Brain metabolism in health, aging, and neurodegeneration. *EMBO J.* 2017;36:1474–1492. doi: 10.15252/embj.201695810 [PubMed: 28438892]
46. Cohen-Cory S, Kidane AH, Shirkey NJ, Marshak S. Brain-derived neurotrophic factor and the development of structural neuronal connectivity. *Dev Neurobiol.* 2010;70:271–288. doi: 10.1002/dneu.20774 [PubMed: 20186709]
47. Phillips C, Baktir MA, Srivatsan M, Salehi A. Neuroprotective effects of physical activity on the brain: a closer look at trophic factor signaling. *Front Cell Neurosci.* 2014;8:170. doi: 10.3389/fncel.2014.00170 [PubMed: 24999318]
48. Zipes DP. Influence of myocardial ischemia and infarction on autonomic innervation of heart. *Circulation.* 1990;82:1095–1105. doi: 10.1161/01.cir.82.4.1095 [PubMed: 2205413]
49. Chidsey CA, Braunwald E, Morrow AG. Catecholamine Excretion and Cardiac Stores of Norepinephrine in Congestive Heart Failure. *Am J Med.* 1965;39:442–451. doi: 10.1016/0002-9343(65)90211-1 [PubMed: 14338295]
50. Yu G, Wang W. Protective effects of LM22A-4 on injured spinal cord nerves. *Int J Clin Exp Pathol.* 2015;8:6526–6532. [PubMed: 26261531]
51. Minichiello L TrkB signalling pathways in LTP and learning. *Nat Rev Neurosci.* 2009;10:850–860. doi: 10.1038/nrn2738 [PubMed: 19927149]
52. Wan R, Weigand LA, Bateman R, Griffioen K, Mendelowitz D, Mattson MP. Evidence that BDNF regulates heart rate by a mechanism involving increased brainstem parasympathetic neuron excitability. *J Neurochem.* 2014;129:573–580. doi: 10.1111/jnc.12656 [PubMed: 24475741]
53. Olshansky B, Sabbah HN, Hauptman PJ, Colucci WS. Parasympathetic nervous system and heart failure: pathophysiology and potential implications for therapy. *Circulation.* 2008;118:863–871. doi: 10.1161/CIRCULATIONAHA.107.760405 [PubMed: 18711023]
54. Pradhan J, Noakes PG, Bellingham MC. The Role of Altered BDNF/TrkB Signaling in Amyotrophic Lateral Sclerosis. *Front Cell Neurosci.* 2019;13:368. doi: 10.3389/fncel.2019.00368 [PubMed: 31456666]
55. Omiya K, Nakadate Y, Oguchi T, Sato T, Matsuoka T, Abe M, Kawakami A, Matsukawa T, Sato H. Cardioprotective effects of enteral vs. parenteral lactoferrin administration on myocardial ischemia-reperfusion injury in a rat model of stunned myocardium. *BMC Pharmacol Toxicol.* 2022;23:78. doi: 10.1186/s40360-022-00619-w [PubMed: 36242077]
56. Gelpi RJ, Morales C, Cohen MV, Downey JM. Xanthine oxidase contributes to preconditioning's preservation of left ventricular developed pressure in isolated rat heart: developed pressure may not be an appropriate end-point for studies of preconditioning. *Basic Res Cardiol.* 2002;97:40–46. doi: 10.1007/s395-002-8386-0 [PubMed: 11998976]
57. Chan CB, Tse MC, Liu X, Zhang S, Schmidt R, Otten R, Liu L, Ye K. Activation of muscular TrkB by its small molecular agonist 7,8-dihydroxyflavone sex-dependently regulates energy metabolism in diet-induced obese mice. *Chem Biol.* 2015;22:355–368. doi: 10.1016/j.chembiol.2015.02.003 [PubMed: 25754472]
58. Hasegawa Y, Suzuki H, Altay O, Zhang JH. Preservation of tropomyosin-related kinase B (TrkB) signaling by sodium orthovanadate attenuates early brain injury after subarachnoid hemorrhage in rats. *Stroke.* 2011;42:477–483. doi: 10.1161/STROKEAHA.110.597344 [PubMed: 21193742]



59. Oeing CU, Jun S, Mishra S, Dunkerly-Eyring BL, Chen A, Grajeda MI, Tahir UA, Gerszten RE, Paolucci N, Ranek MJ, et al. MTORC1-Regulated Metabolism Controlled by TSC2 Limits Cardiac Reperfusion Injury. *Circ Res.* 2021;128:639–651. doi: 10.1161/CIRCRESAHA.120.317710 [PubMed: 33401933]
60. Pharoah BM, Khodade VS, Eremiev A, Bao E, Liu T, O'Rourke B, Paolucci N, Toscano JP. Hydropersulfides (RSSH) Outperform Post-Conditioning and Other Reactive Sulfur Species in Limiting Ischemia-Reperfusion Injury in the Isolated Mouse Heart. *Antioxidants (Basel).* 2022;11. doi: 10.3390/antiox11051010
61. Solari A, Finos L, Goeman JJ. Rotation-based multiple testing in the multivariate linear model. *Biometrics.* 2014;70:954–961. doi: 10.1111/biom.12238 [PubMed: 25269416]
62. Goeman JJ, Solari A. Multiple hypothesis testing in genomics. *Stat Med.* 2014;33:1946–1978. doi: 10.1002/sim.6082 [PubMed: 24399688]

**Novelty****What Is Known?**

- BDNF (via TrkB) is essential for proper heart development/function.
- BDNF levels are elevated early after ischemia.
- Neuronal BDNF protects the heart against ischemic injury
- TrkB agonists are beneficial early after MI.

**What New Information Does this Article Contribute?**

- Cardiac BDNF levels decline when chronic post-ischemic LV dysfunction ensues
- TrkB agonists promote neurite growth/angiogenesis and enhance myocyte function
- LM22A-4 arrests CHF progression limiting myocyte apoptosis, and loss of cardiac neurons/vessels
- Myocyte-specific BDNF deletion exacerbates I/R injury
- $\beta$ 3AR stimulation enriches cardiomyocytes with BDNF, protecting the heart against I/R injury: this effect is lost in myoBDNF KO mice
- Metoprolol enriches infarcted myocytes with BDNF

**Significance**

BDNF/TrkB signaling is essential for heart development and adult function. We show that, after ischemia, cardiomyocytes generate BDNF via TrkB and  $\beta$ 3AR stimulation. This phenomenon declines in mice with heart failure (HF) because of  $\beta$ 3AR down-regulation. TrkB agonists arrest post-ischemic HF progression, enhancing myocyte function and rescuing cardiac innervation/vascularity: effects lost in  $\beta$ 3AR or myoBDNF KO mice. Myocardial BDNF generation is part of a beneficial loop: circulating BDNF - sarcolemmal TrkB stimulation – myocyte BDNF production. The latter will exert autocrine and paracrine effects on neighboring myocardial structures. TrkB agonists potentially can counter chronic post-ischemic HF.

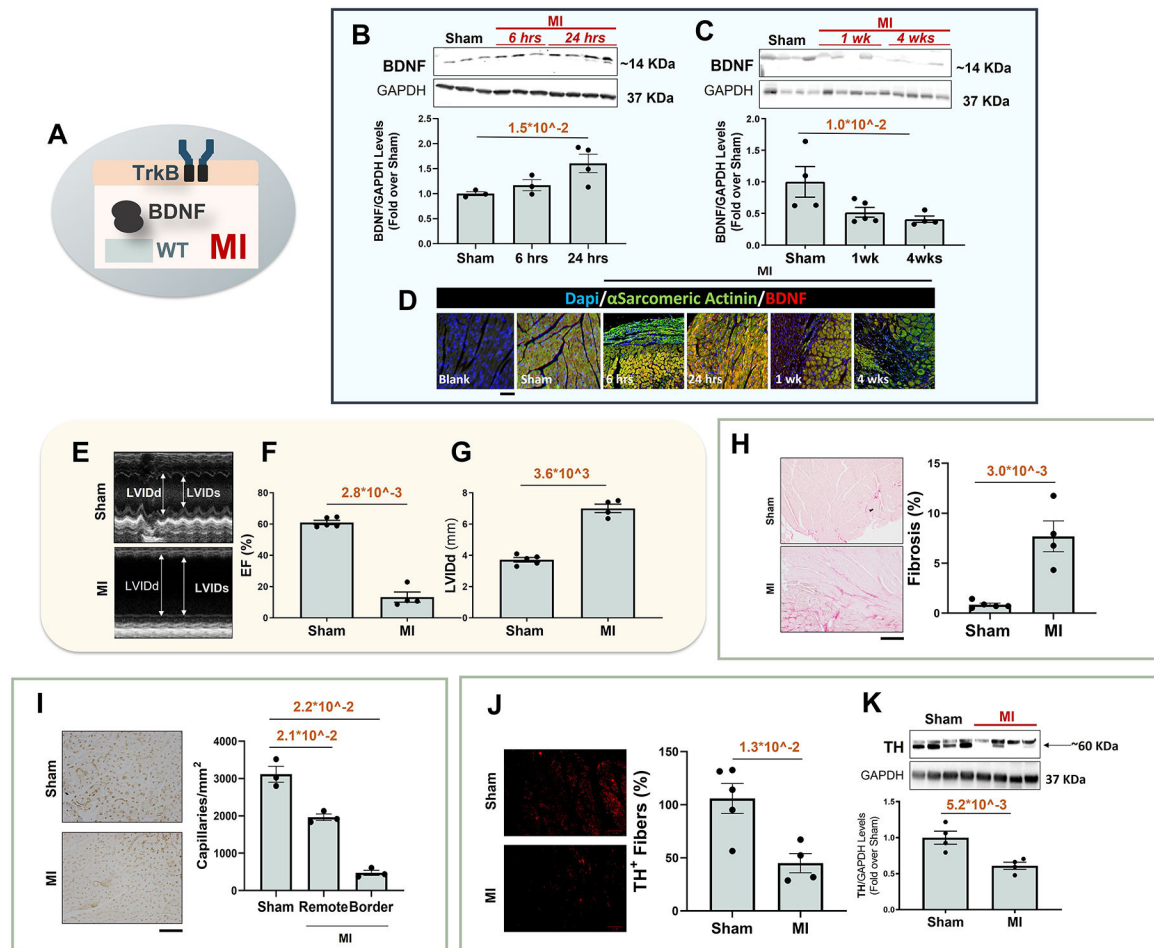


**Figure 1. Post-ischemic LV dysfunction is coupled with lower cardiac BDNF content and associated with reduced cardiac sympathetic nerve fibers and poor vascularization.**

**A)** Mouse genotype: WT; Intervention: MI; **B-C)** Representative immunoblots/densitometric quantitative analysis of multiple independent experiments to evaluate BDNF expression levels, in total cardiac lysates of 6 hours (hrs) and 24 hrs (sham n=3, 6 hrs n=3, and 24 hrs n=4) (**B**) or 1 week and 4 weeks (sham n=4, 1wk n=5, and 4wks n=4) (**C**) post-MI mice. Sham-operated animals were used as control. GAPDH levels were used as loading control. **D)** Representative panels (merge) of DAPI (blue),  $\alpha$ -sarcomeric actinin staining (green), and BDNF (red) immunofluorescence images (scale bar, 50  $\mu$ m) showing data concerning BDNF expression in cardiac sections from sham, 6 hrs, 24 hrs, 1 and 4 weeks post-MI mice; **E-F-G)** Representative images of echocardiographic analysis (M-mode) performed at 4 weeks post-MI and dot plots showing **F)** left ventricle (LV) ejection fraction (EF, %) (sham n=5, and MI n=4), **G)** LV internal diameter at diastole (LVIDd, mm) (sham n=5, and MI n=4) of individual mice from each of the groups: sham and MI. **H)** Representative images/aquantitative data of percent cardiac fibrosis (Picro-Sirius red staining, Scale bar 200  $\mu$ m) in cardiac sections from sham and MI mice (sham n=5, and MI n=4). **I)** Representative images of *Lectin Bandeiraea simplicifolia I* staining of capillaries in the ischemic vs. sham-operated myocardium (scale bar: 200  $\mu$ m, left panels); and a bar graph showing capillary/mm<sup>2</sup> in cardiac sections of sham and MI mice (sham n=3, MI remote n=3, and MI border n=3).

**J)** Representative images/quantitative data of percent tyrosine hydroxylase (TH) positive (+) fibers (immunofluorescence staining, scale bar (50  $\mu$ m) in cardiac sections from sham and MI mice (sham n=5, and MI n=4). **K)** Representative immunoblots/densitometric quantitative analysis of TH protein level in total cardiac lysates of sham and MI mice (sham n=4, and MI n=4). GAPDH levels were used as a loading control. Data were analyzed utilizing a nonparametric rank-based test with Shaffer post hoc correction (B, C, I, F, G, H, J, and K). All data are shown as mean $\pm$ s.e.m.

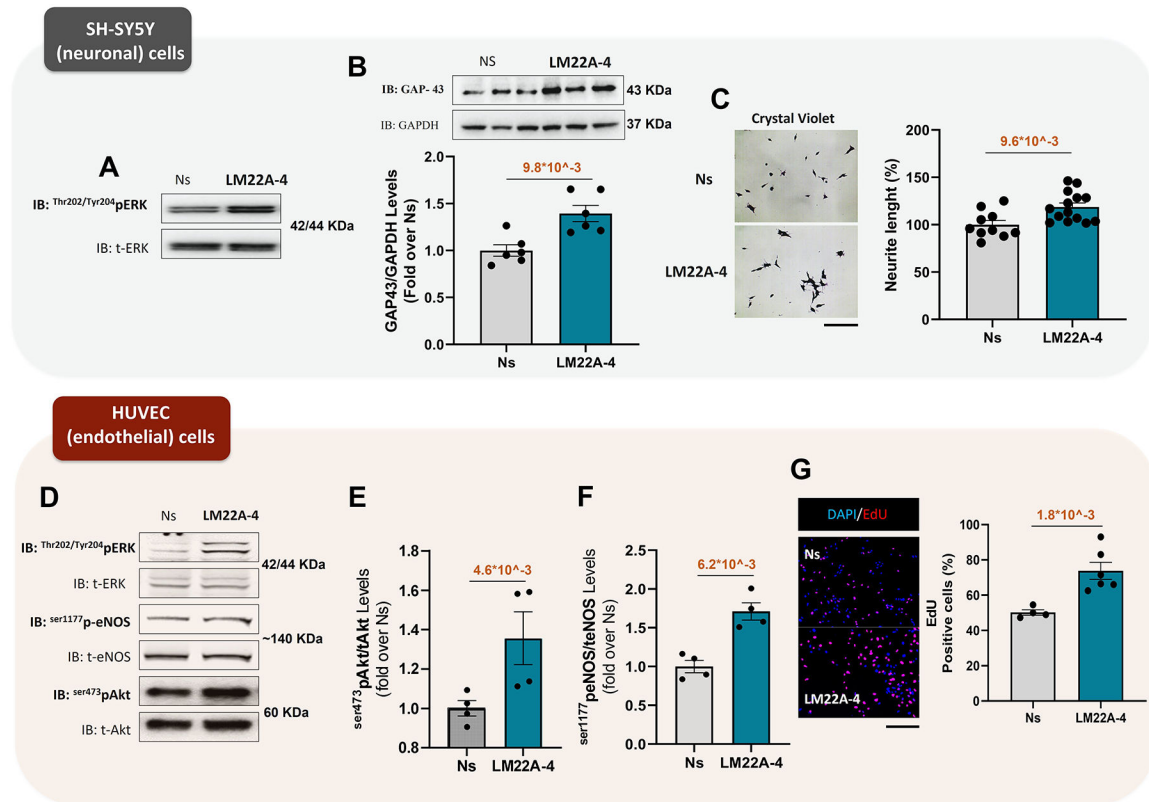


**Figure 2. TrkB-agonism via LM22A-4 enhances neuronal and endothelial cell function, in vitro.**

**A)** Representative immunoblots showing ERK activation (phospho-Thr202/Tyr204) in total lysates from SH-SY5Y neuronal cell lysates unstimulated (Ns) or stimulated with LM22A-4 (100 nM) for 10 min. Total ERK (t-ERK) levels were used as loading control.

**B)** Representative immunoblots/densitometric quantitative analysis of GAP-43 levels in total lysates from SH-SY5Y neuronal cell lysates Ns or stimulated with LM22A-4 (100 nM) for 24 hours (Ns n=6, and LM22A-4 n=6). GAPDH levels were used as loading control.

**C)** Representative images/quantitative data showing neurite length percentage (%) in SH-SY5Y Ns or stimulated with LM22A-4 (100 nM) for 24 hours (Ns n=10, LM22A-4 n=14).

**D-E-F)** Representative immunoblots (**D**) and densitometric quantitative analysis (**E-F**) showing ERK activation (phospho-Thr202/Tyr204) (**D**); Akt activation (phospho-ser473) (**E**) and eNOS activation (phospho-ser1177) levels (**F**) in total lysates from HUVEC lysates Ns or stimulated with LM22A-4 (100 nM) for 10 min (Ns n=4, and LM22A-4 n=4). Total ERK (t-ERK), tAkt, and eNOS levels were used as the loading control, respectively.

**G)** Representative images/quantitative data of the EdU positive cell percentage (%) (immunofluorescence staining, scale bar (200 μm) in HUVEC cells. Ns or stimulated with LM22A-4 (100 nM) for 12 hours (Ns n=4, and LM22A-4 n=6). Data were analyzed via a nonparametric rank-based test with Shaffer post hoc correction (B, E, F, G, and C). All data are shown as mean±s.e.m.

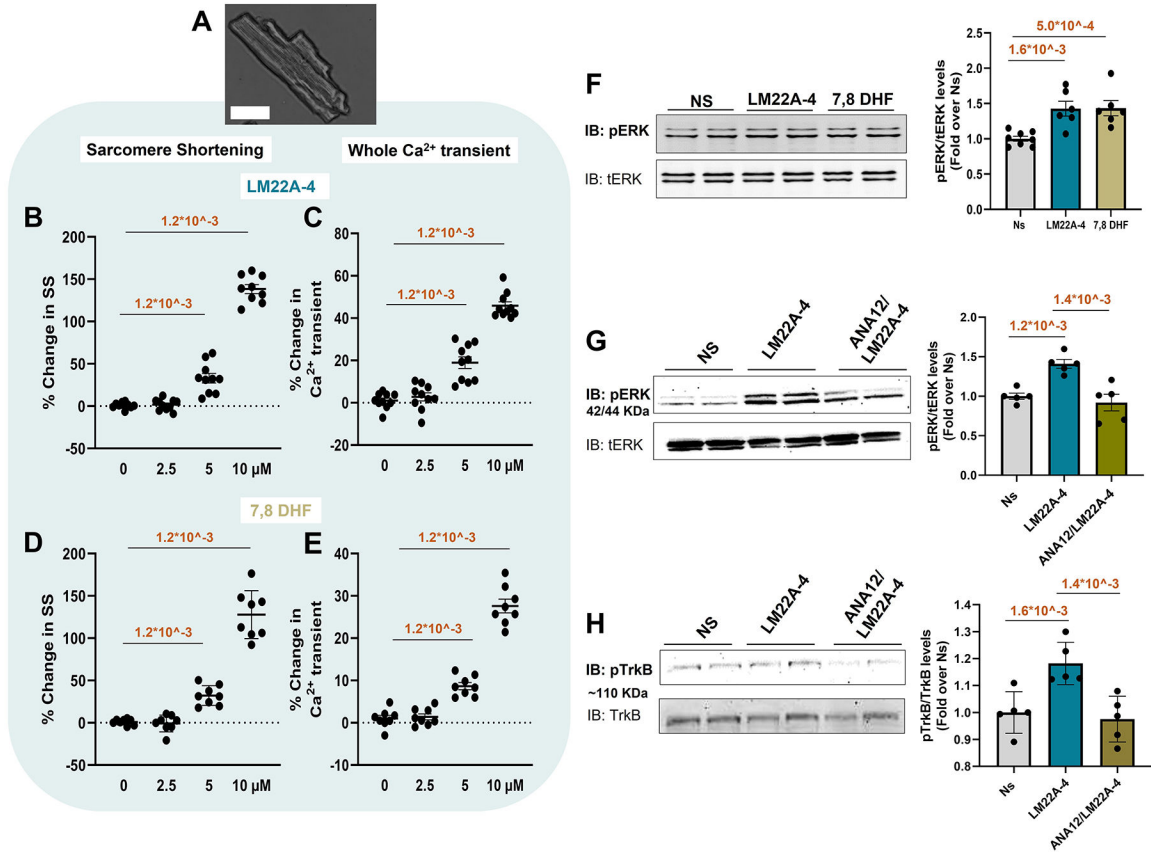


**Figure 3. LM22A-4 and 7,8-DHF enhance inotropy and whole calcium transient in isolated adult murine cardiomyocyte via TrkB activation.**

**A-C)** Representative image of adult murine isolated cardiomyocyte (scale bar 25  $\mu$ m) (**A**) and quantitative data showing percentage change of sarcomere shortening (**B**) and percentage change of calcium transient (**C**) of isolated cardiomyocytes unstimulated (0  $\mu$ M; n=10) or stimulated with LM22A-4 at 2.5  $\mu$ M (n=10), 5  $\mu$ M (n=10), and 10  $\mu$ M (**B**, n=9 and **C**, n=10) **D-E**) Quantitative data showing percentage change of sarcomere shortening (**D**) and percentage change of calcium transient (**E**) of isolated cardiomyocytes unstimulated (0  $\mu$ M) or stimulated with 7,8-DHF at 2.5  $\mu$ M, 5  $\mu$ M, and 10  $\mu$ M (0  $\mu$ M n=8, 2.5  $\mu$ M n=8, 5  $\mu$ M n=8, and 10  $\mu$ M n=8). **F**) Representative immunoblots and densitometric quantitative analysis showing ERK activation (phospho-Thr202/Tyr204) in total lysates from NRVMs Ns or stimulated with LM22A-4 (100 nM) or 7,8-DHF (100 nM) for 10 min (Ns n=8, LM22A-4 n=6, and 7,8-DHF n=6). Total ERK (tERK), levels were used as the loading control. **G-H**) Representative immunoblots and densitometric quantitative analysis showing (**G**) ERK activation (phospho-Thr202/Tyr204) and (**H**) TrkB phosphorylation (phospho-Tyr816) levels in total lysates from NRVMs Ns or stimulated with LM22A-4 (100 nM) for 10 min. Prior LM22A-4 stimulation a group of cells was pre-treated with ANA-12 (10  $\mu$ M) for 30 min. (Ns n=5, LM22A-4 n=5, and A12/LM22A-4 n=5). Total ERK (tERK), levels were used as the loading control. Data were analyzed employing a nonparametric rank-based test with Shaffer post hoc correction (B, D,C, E, F, G, and H). All data are shown as mean $\pm$ s.e.m.



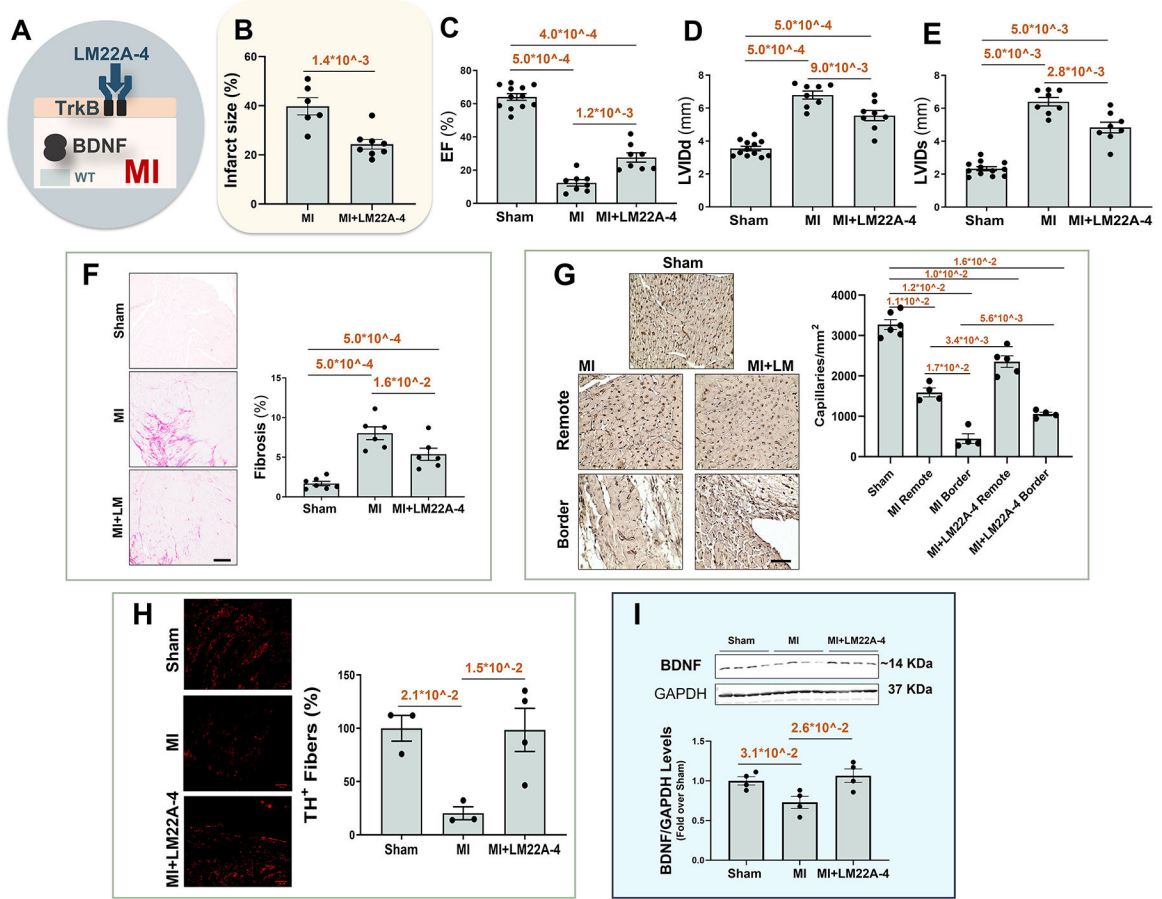


**Figure 4. In vivo TrkB-agonism prevents chronic post-ischemic cardiac decompensation and increases myocardial BDNF content.**

**A)** Mouse genotype: WT; Interventions: MI  $\pm$  LM22A-4; **B)** Dot plots showing the percentage of infarct size evaluated 4 weeks post-MI in mice treated with vehicle (saline solution, MI) or LM22A-4 (MI n=6, and MI+LM22A-4 n=8). **C-D-E)** Dot plots showing the echocardiographic analysis performed at 4 weeks post-MI (**C**) LV ejection fraction (EF, %), (**D**) LV internal diameter at diastole (LVIDd, mm), (**E**) LV internal diameter at systole (LVIDs, mm) (sham n=12, MI n=8, and MI+LM22A-4 n=8). **F)** Representative images/quantitative data showing the percentage of cardiac fibrosis (Picro-Sirius red staining, scale bar 200  $\mu$ m) in cardiac sections from sham, MI, and MI+LM22A4 mice (sham n=7, MI n=6, and MI+LM22A-4 n=6). **G)** Representative images of Lectin Bandeiraea simplicifolia I staining of capillaries in the ischemic vs. sham-operated myocardium (scale bar: 200  $\mu$ m) and a bar graph showing capillary/mm<sup>2</sup> in cardiac section of sham, MI and MI+LM22A-4 mice (sham n=6, MI remote n=4, MI border n=4, MI+LM22A-4 remote n=5, and MI+LM22A-4 n=4). **H)** Representative images/quantitative data of TH<sup>+</sup> fiber percentage (immunofluorescence staining, scale bar (50  $\mu$ m) in cardiac sections from sham, MI and MI+LM22A-4 mice (sham n=3, MI n=3, and MI+LM22A-4 n=4). **I)** Representative immunoblots/densitometric quantitative analysis showing of BDNF levels in total cardiac lysates of MI and MI+LM22A4 mice (sham n=4, MI n=4, and MI+LM22A-4 n=4). GAPDH levels were used as a loading control. Data were analyzed using a nonparametric rank-based

test with Shaffer post hoc correction (B, C, D, E, F, G, H, and I). All data are shown as mean±s.e.m.

Author Manuscript

Author Manuscript

Author Manuscript

Author Manuscript

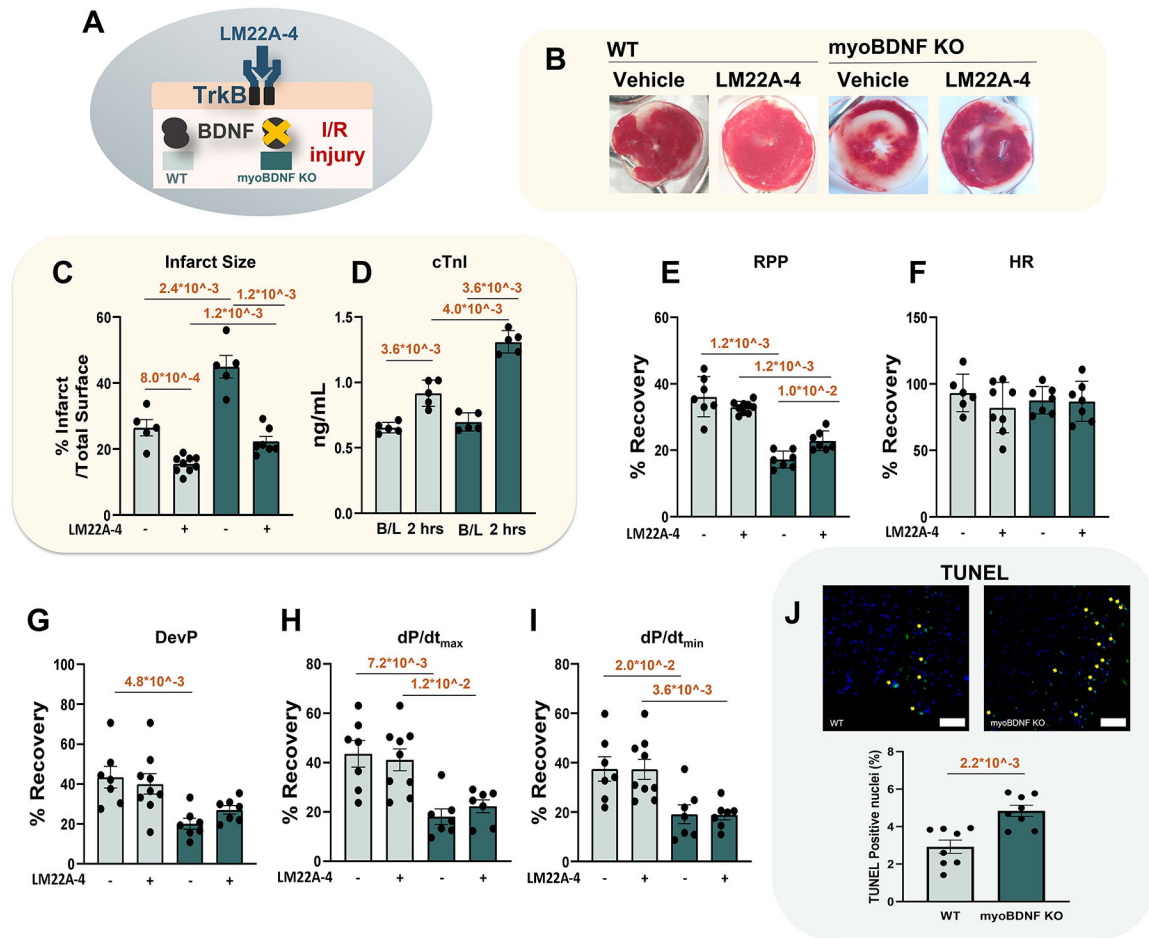


**Figure 5. Ex Vivo TrkB agonism limits infarct size and cardiac functional deterioration post-ischemia-reperfusion injury.**

**A)** Mouse genotypes: WT and myoBDNF KO; Interventions: I/R injury  $\pm$  LM22A-4; **B-C)** Representative images of I/R induced infarct size (**B**) and quantitative data of the infarct size (**C**) by global ischemia via Langendorff perfusion with or without LM22A-4 (20  $\mu$ M) during the first 10 minutes of reperfusion. (WT n=5, WT+LM22A-4 n=9, myoBDNF KO n=5, and myoBDNF KO+LM22A-4 n=7). **D)** Quantitative data showing cTnI release in the coronary effluent. (WT Baseline n=5, WT 2 hrs reperfusion n=5, myoBDNF KO Baseline n=5, and myoBDNF KO 2 hrs reperfusion n=5). **(E)**, heart rate (**F**), LV developed pressure (**G**),  $dP/dt_{max}$  (**H**), and  $dP/dt_{min}$  (**I**) post I/R injury via Langendorff perfusion with or without LM22A-4 (20  $\mu$ M) during the first 10 minutes of reperfusion. (WT n=7, WT+LM22A-4 n=9, myoBDNF KO n=7, and myoBDNF KO+LM22A-4 n=7). **J)** Representative images of TUNEL assay and quantitative data showing the percentage of TUNEL positive cells (%) (immunofluorescence staining, scale bar (50  $\mu$ m) in I/R induced hearts of WT and myoBDNF KO. (WT n=8, and myoBDNF KO n=8). Data were analyzed utilizing a nonparametric rank-based test with Shaffer post hoc correction (C, D, E, G, H, I, and J). All data are shown as mean  $\pm$  s.e.m.

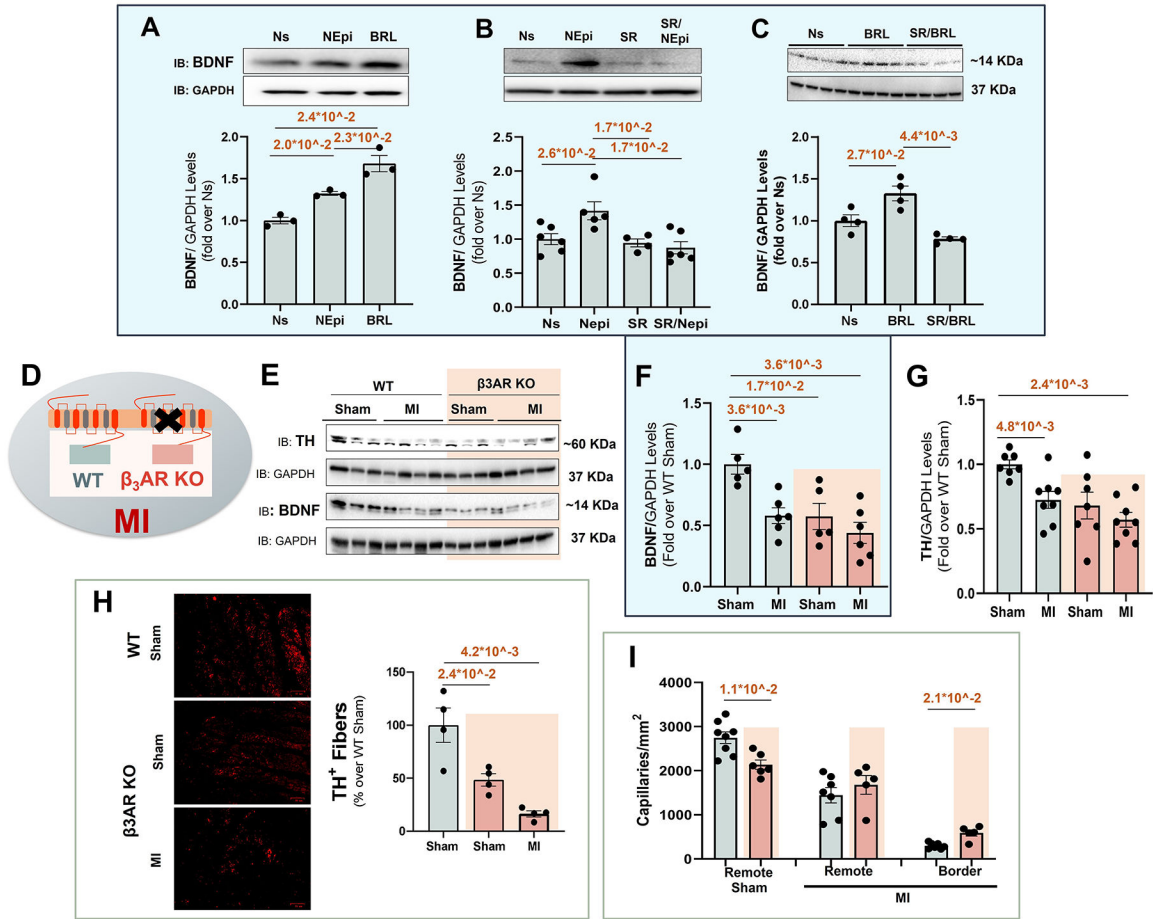


**Figure 6. In ischemic CHF, disrupted  $\beta_3$ AR-signaling accounts for BDNF expression loss, reduced cardiac sympathetic innervation, and angiogenesis.**

**A)** Representative immunoblots and densitometric quantitative analysis showing levels of BDNF in total lysates from NRVMs unstimulated (Ns) or stimulated with NEpi (10  $\mu$ M) or BRL-37344 (BRL, 1  $\mu$ M) for 12 hrs. GAPDH was the loading control. (Ns n=3, Nepi n=3, and BRL n=3). **B)** Representative immunoblots/densitometric quantitative analysis of BDNF levels in total lysates from unstimulated (Ns) or NEpi-stimulated (10  $\mu$ M for 12 hrs) NRVMs. Prior NEpi treatment, a group of cells was pre-treated with SR59230A (SR, 10  $\mu$ M) for 30 min. GAPDH was the loading control. (Ns n=6, Nepi n=5, SR n=4, and SR/Nepi n=6). **C)** Representative immunoblots/densitometric quantitative analysis of BDNF levels in total lysates from NRVMs unstimulated (Ns) or stimulated with BRL (1  $\mu$ M) for 12 hrs. Prior BRL treatment a group of cells were pre-treated with SR59230A (SR, 10  $\mu$ M) for 30 min. GAPDH was used as loading control. (Ns n=4, BRL n=4, and SR/BRL n=4). **D)** Mouse genotypes: WT and  $\beta_3$ AR KO mice; Intervention: MI. **E-F-G)** Representative immunoblots (**E**) and densitometric quantitative analysis (**F-G**) showing BDNF and TH levels in total cardiac lysates from the following groups: WT (sham and MI) and  $\beta_3$ AR KO (sham and MI) mice. GAPDH levels were used for protein loading controls. **F)** BDNF: WT sham n=5, WT MI sham n=6,  $\beta_3$ AR KO sham n=5, and  $\beta_3$ AR KO MI n=6 and **G)** TH: WT sham n=7, WT MI sham n=8,  $\beta_3$ AR KO sham n=7, and  $\beta_3$ AR KO MI n=8. **H)** Representative images/quantitative data of TH<sup>+</sup> fiber percentage (immunofluorescence staining, scale bar

(50  $\mu\text{m}$ ) in cardiac sections from sham, MI (WT *vs.*  $\beta$ 3AR KO) mice (WT sham  $n=4$ ,  $\beta$ 3AR KO sham  $n=4$ , and  $\beta$ 3AR KO MI  $n=4$ ). **I**) Representative images of Lectin Bandeiraea simplicifolia I staining of capillaries in the ischemic *vs.* sham-operated myocardium (scale bar: 200  $\mu\text{m}$ ) and bar graph showing capillary/ $\text{mm}^2$  in cardiac section from sham and MI (WT *vs.*  $\beta$ 3AR KO) mice (WT remote sham  $n=8$ ,  $\beta$ 3AR KO remote sham  $n=6$ , WT remote MI  $n=7$ ,  $\beta$ 3AR KO remote MI  $n=5$ , WT border MI  $n=7$ , and  $\beta$ 3AR KO border MI  $n=5$ ). Data were analyzed using a nonparametric rank-based test with Shaffer post hoc correction (A, B, C, F, G, H, and I). All data are shown as mean $\pm$ s.e.m.

Author Manuscript

Author Manuscript

Author Manuscript

Author Manuscript

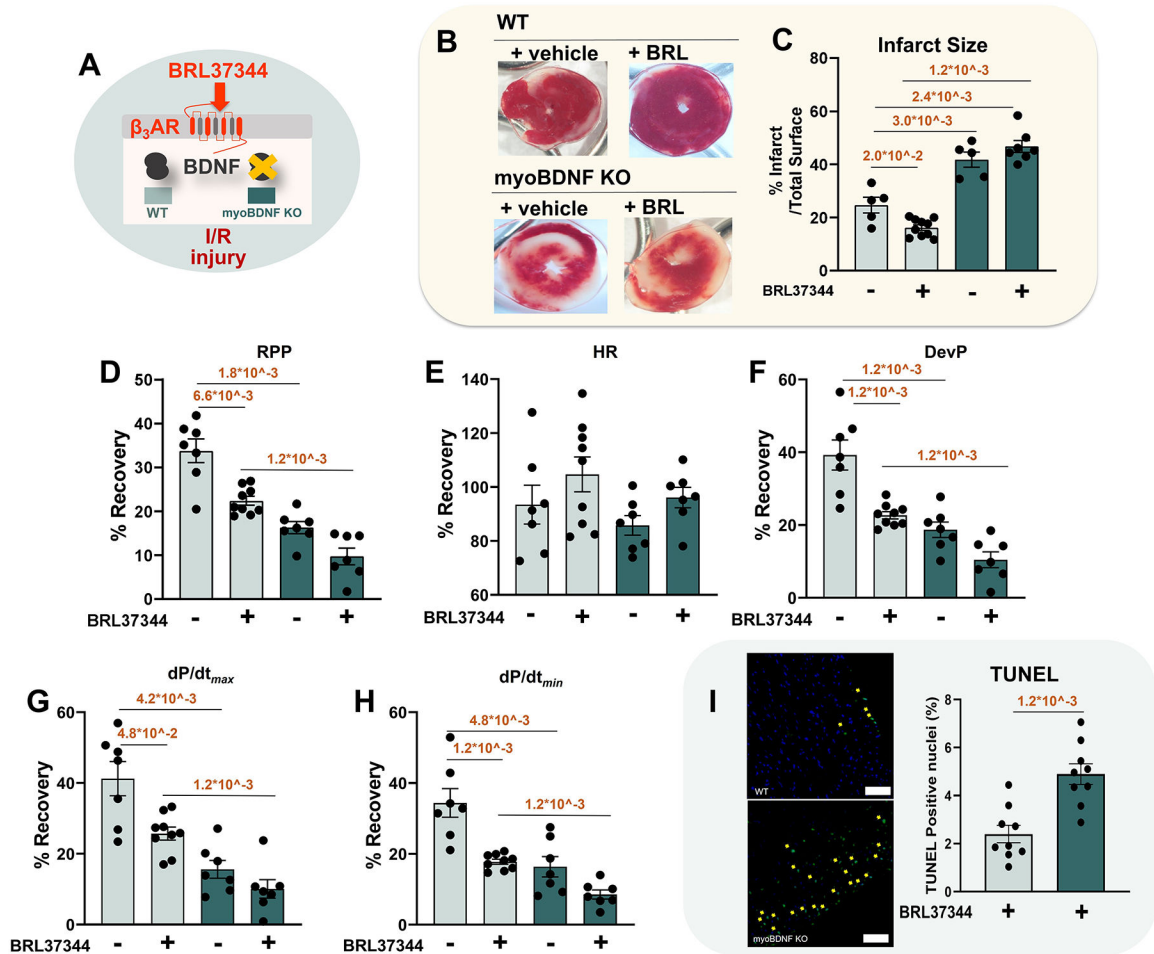


**Figure 7. In I/R injured hearts,  $\beta_3$ AR benefits require cardiomyocyte borne BDNF.**

**A)** Mouse genotypes: WT and myoBDNF KO; Interventions: I/R injury  $\pm$ BRL-37344.

**B-C)** Representative images of I/R induced infarct size (TTC staining) (**B**) and quantitative data of the infarct size (**C**) by global ischemia via Langendorff perfusion with or without BRL37344 (10  $\mu$ M) during first 10 minutes of reperfusion (WT n=5, WT+BRL37344 n=10, myoBDNF KO n=5, and myoBDNF KO+BRL37344 n=7). **D-H)** Quantitative data showing percentage recovery of rate-pressure product (**D**), heart rate (**E**), LV developed pressure (**F**),  $dP/dt_{max}$  (**G**) and  $dP/dt_{min}$  (**H**). (WT n=7, WT+BRL37344 n=9, myoBDNF n=7, and myoBDNF+BRL37344 n=7). **(I)** Representative images/quantitative data of TUNEL positive cell percentage (%) (immunofluorescence staining, scale bar (50  $\mu$ m) in I/R induced hearts of WT and myoBDNF KO with BRL37344. (WT+BRL37344 n=9, and myoBDNF KO+BRL37344 n=9). Data were analyzed via a nonparametric rank-based test with Shaffer post hoc (C, D, GF, H, and I). All data are shown as mean $\pm$ s.e.m.



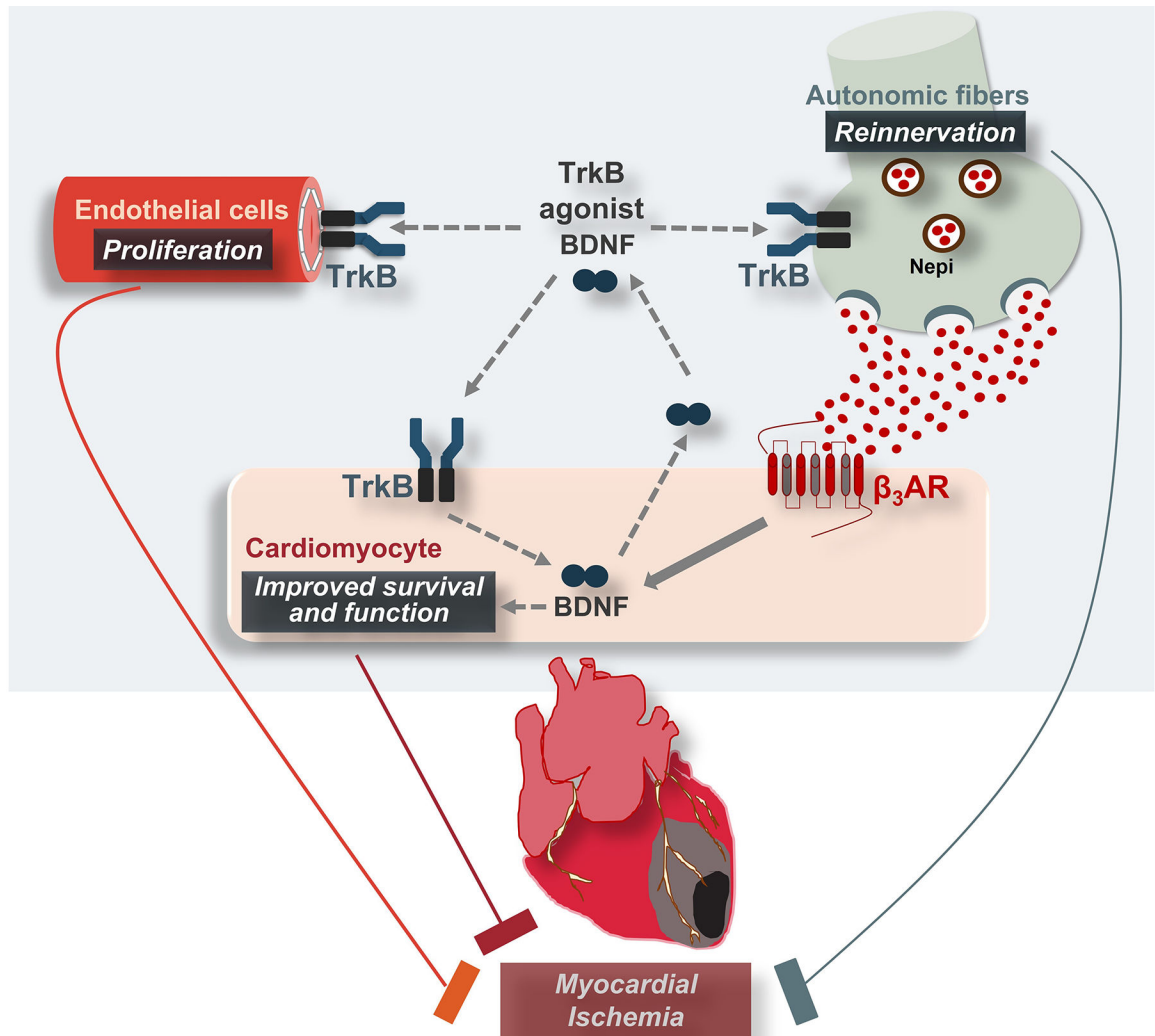


**Figure 8. Synopsis of the findings/Conceptual framework of the study.**

TrkB agonism and  $\beta_3$ AR-induced BDNF production arrest post-ischemic CHF progression, exerting myocardial autocrine/paracrine protective effects: 1) inducing a therapeutic response in ischemic cardiomyocytes, i.e., limiting cell death and improving function; 2) activating endothelial cell proliferation, and 3) enhancing autonomic neuronal sprouting.